

Air and Underwater Sound Emission by Drop Impact on the Free Surface

Yu.D. Chashechkin¹, V.E. Prokhorov²

A. Ishlinskii Institute for Problems in Mechanics of the RAS, Moscow, Russia

*¹chakin@ipmnet.ru; ²prohorov@ipmnet.ru

Received 16 February 2013; Accepted 16 May 2013; Published 18 February 2014

© 2014 Science and Engineering Publishing Company

Abstract

A drop falling onto a free water surface produces acoustic packets propagating both in the air and underwater. The high-frequency shock pulse usually follows the impact accompanied by two or more acoustic packets. In experiments, the sound signals and video recording of the flow in the drop impact area were carried out simultaneously. Comparative analysis of the video- and acoustic records disclosed a strong temporal correlation between air cavities detaching from the underwater cavern and sound signals. The sounds arise to the moments when the cavities tear off the cavern and stop when the cavities shape to regular (elliptical or spherical) forms.

Keywords

Drop; Cavern; Cavity; Sound Packet; Shock Pulse; Microphone; Hydrophone; Recording; Correlation

The processes following impact of the drop on the free water surface were first studied in the middle of 19th century when circular vortex ring produced by falling dyed drop was observed (Rogers V.B., 1858). Later the process of drop impact was investigated using electric spark photography in new details (Thomson J.J., Newall H.F., 1885).

The excellent photographic study by Worthington (1908) revealed that reach family of well-reproduced fast flow components accompanying drop fall onto deep fluid surface, including caverns, crowns, splashes and capillary waves.

Since about 20th of the last century, a sound emission produced by falling drop has been observed by a number of scientists, firstly in the air where musical nature of sound was identified (Jones A.T., 1920). Later the monotonic beeping of drop impact was attributed to resonant oscillations of the entrained air bubbles. Based on this hypothesis Minnaert (1933) suggested a simple formula defining a frequency of volume resonant oscillation of the bubble, which has

been widely used up till now (Prosperetti A., Oguz H.N., 1993).

(Minnaert M., 1933) frequencies corresponded to natural oscillation frequencies of gas bubbles. The simple relation between emitted sound frequency and radius of the spherical bubble has been used up to nowadays.

The hydrophones deployed into marine environment for detection of submarines during World War II reveal reach underwater acoustic noise. Among the noise sources breaking waves, wind, marine shipping, life, and rain were disclosed. Empirical spectral shape of the noise over the band 0.5 – 25 kHz was suggested to select wind generated noise, (Knudsen V. O., Alford R. S., Emling J. W., 1948). Later it was found that this frequency range includes singular maximum within 15 kHz of the noises produced by heavy rain (Nystuen J. A., 1986). The spectral maximum was also identified in the sound energy radiated into the water by the splashes of single water droplets (Franz G.J., 1959).

Experimental study of the acoustic noise produced by drop impact has been widely carried out in the 80th and in 90th numerous data on the spectra shape of underwater noise due to natural as well as artificial rain which confirmed a prominent peak at frequency about 14 kHz caused by sound emission by the bubbles entrained in the liquid during the impact of rain drops. Prominence of the spectral peak indicates that the sizes of sounding bubbles groups within narrow range of values (Prosperetti A., Crum L.A., Pumphrey H. C., 1989).

Precise laboratory experiments revealed that drop splash sound was produced in two ways: firstly, when the drop touches the surface, and, secondly, when an air bubble appears in the water. The shock sound was emitted in every drop contact, the second occurs for some drop impact but not for each one (Pumphrey H.

C., Crum L.A., Bjorno L. 1989). Subsequent experiments demonstrated that sound is emitted not only by water drops, but also by slowly falling snowflakes (Crum L.A., Pumphrey H. C., Roy R.A., Prosperetti A., 1999).

An overview of the main results concerning flow pattern observed during the drop impact in fluids and underwater noise of rain was given in two papers. Physics of fluid flows, acoustic of the impact and allied phenomena have been discussed in (Prosperetti A., Oguz H.N., 1993). The noise spectra and interpretation of their relations to the rain drop size and impact mechanism were presented by L. Bjorno (1994).

Fresh experiments confirmed the typical sequence of the sound signals produced by the drop containing a shock pulse and intensive sound packet following after large delay (150 – 200 ms) (Prokhorov V.E., Chashechkin Yu.D., 2011a). However, as it was revealed in many experiments with drops of enlarged size (about 0.5 cm), the shock pulse is accompanied by series (from 2 to 4) of sound packets. Variety of sound packets numbers produced by single drop testify to complexity and variability of mutually connected hydrodynamic and acoustic processes caused by drop fall. This demands to observe all the complex of the phenomena instantaneously with high spatial and temporal resolutions.

Dynamics of the cavern and the upward stream and the cascade of flows propagating on the surface and in the bulk of a fluid continue to attract the attention of physicists owing to their abundance in nature and importance of practical applications, particularly acoustic ones due to development of the ocean remote sensing. The aim of this work is to study the mutual relations between hydrodynamic and acoustic processes accompanying a drop falling in a liquid using a fast speed video recording and registration of the sound pressure in the air and water.

Dimensional and Dimensionless Parameters of the Phenomena

In current experiments, a drop of the water fell free into the tank filled with the same water. The fluid is characterized by density ρ , kinematic viscosity ν , and surface tension coefficient σ . The drop has diameter D , surface S and volume V defining the drop m . The drop falling from a height H at the instant of contact has velocity U , momentum $p = mU$, and kinetic energy $E = mU^2/2$ and surface energy $E_s = \sigma S$ being a part of internal energy.

The surface of the drop was not perfect and can be distorted by volume oscillations and capillary waves arose during drop separation from the nozzle. The frequency of volume oscillations in the ideal fluid approximation was examined in (Rayleigh, 1877). The shape of the drop depends on its size and velocity defining the air drag and interaction with stagnant air. The shape can be changed from spherical to bell-shaped (Villermaux E., Bossa B., 2009).

In description of the drop impact and subsequent processes large number of parameters are used from which the basic are numbers of Weber $We = \rho U^2 D / \sigma$, Bond $Bo = \rho D^2 / \sigma$ and Reynolds $Re = UD / \nu$. In number of papers Ohnesorge $Oh = \sqrt{\rho \nu / \sigma D} = \sqrt{We} / Re$ and Froude number $Fr = U^2 / gD$ are used, where g is gravity acceleration.

To characterized acoustic phenomena Mach number $Ma = U / c$, where c is sound velocity, is commonly used. As is generally accepted, the sounding sources are small gas bubbles involved into liquid during the drop impact. An efficiency of such sources depends on ratio between bubble size D and wavelength λ of emitted sound packet.

The experiments were conducted under constant ambient conditions (temperature, pressure, humidity), so the kinetic and thermodynamic parameters are supposed to be constant.

The problem is characterized by two time scales conditioned by difference in time of exchange of mechanic and internal energy as a part of total energy. The first component is defined by the time of drop sinking into the underlying liquid, which is $\tau_m = D / U$ an order of magnitude. The variance of internal energy $\varepsilon = 2\sigma S$ is determined by short time when the part of the fluid free surface S is eliminated during initial contact of the drop with the surface of target fluid.

Within a short time $\tau_s = \left(\frac{1}{S} \left| \frac{dS}{dt} \right| \right) \ll \tau_m$, disappeared

part of the internal energy is rapidly converted into pressure perturbations, leading to the generation of initial sound pulse and latent flows in the water interior supplementing other kind of flows which manifests itself in deformation of the free surface.

Recoding the pressure fluctuations associated with such fast processes needs in an instrument with high temporal resolution as is ordinary used a high-frequency hydrophone.

The spatial and temporal scales of the phenomenon determine the requirements on the spatial and temporal resolution of the recording device and on the conditions for synchronizing optic and acoustic devices. With these requirements taken into account the experimental technique was developed.

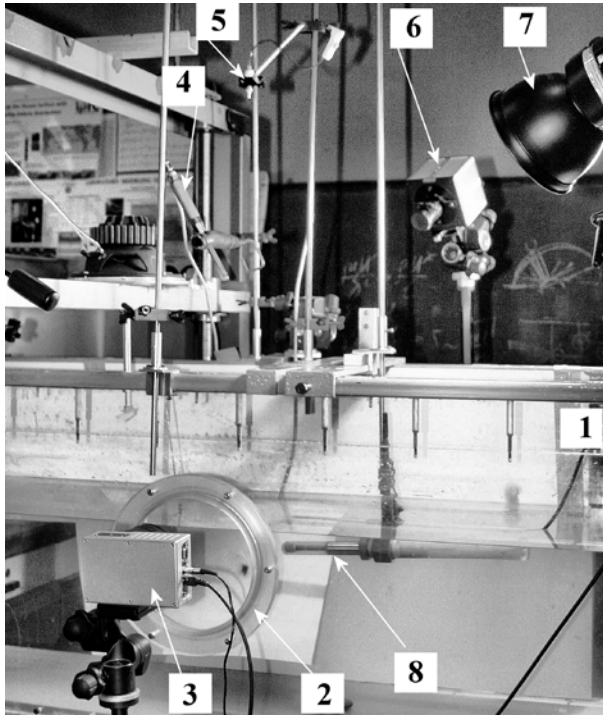


FIG.1 SETUP VIEW: (1) – HYDROOPTICAL TANK, (2) – VIEWING WINDOW, (3) – HIGH SPEED CAMERA "OPTRONIS CR300x2", (4) – MICROPHONE, (5) – DROP EJECTOR NOZZLE, (6) – HIGH SPEED CAMERA "FASTCAM-1024 PCI", (7) – LIGHTER, (8) – HYDROPHONE.

Experimental Setup

View of the stand on which the experiments were conducted is shown in Fig.1. The principal part of the stand is hydrooptical tank 1 $145 \times 50 \times 60$ cm in dimensions with high-quality glass viewing windows 2 (23 cm in diameter) filled with degassed tap water. The depth of water in the tank was 40 cm.

Fast flows were registered by Optronis CR3000x2 high-speed video camera 3 (CCD sensor 13.57×13.68 mm, maximum frame rate 100000 fps, 8 GB internal memory, maximum image size 3 megapixels). The lens axis of camera 3 was nearly horizontal that provides simultaneous observation both underwater and free-surface area of drop impact.

Above the tank sensitive MV-101 microphone 4 (0.02–40 kHz passband, 1.6 V/Pa sensitivity, passband ripples 3 dB at least) was placed for recording sound signals in the air.

The drops were ejected by dispenser 5 placed at height H above the water surface. A set of dispenser nozzles provides the drops of different sizes. In the experiments, the nozzle diameter was 0.4 cm that provides a drop of 0.5 cm across. Within the parameter range of the experiment, the drop was of spherical shape.

General flow pattern on the liquid surface was registered by Photron-1024 PCI camera 6. In current experiments, the frame rate of both cameras was from 2000 to 20000 fps.

The impact area was illuminated by lighter 7 RayLab Xenos RH 1000.

Basic instrument to measure was precision hydrophone 8 (GI51B-type, 30 mV/Pa over 0.002-120 kHz passband with 3 dB of ripples) supplied with a cylindrical sensing element and preamplifier was submerged into the tank.

Data acquisition from sensors of various types, synchronization and pre-processing was performed by special interface unit. The unit performs 12-bit analogue-to-digital conversion and dispatching the data to computer with a clock speed of up to 10 MHz. This provides synchronization video- and acoustic records with accuracy at least $1 \mu\text{s}$ both for separate and delayed starts of camera 3 and interface unit.

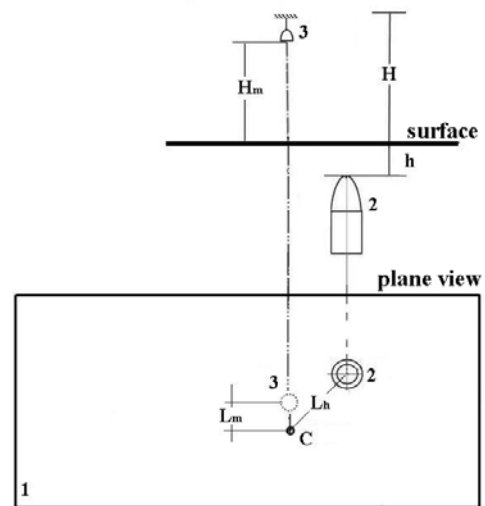


FIG.2 GEOMETRY OF THE EXPERIMENT: (1) TANK, (2) HYDROPHONE, (3) MICROPHONE. $H_m = 22$, $h = 4$, $L_m = 7$, and $L_h = 6$ cm.

Falling drop crossing a laser beam produces the signal starting simultaneously interface unit for registration hydrophone/microphone outputs and cameras. So, sound records were obtained in the air and underwater media concurrently with videorecording

of the drop impact area, as distinct from earlier experiments conducted with separate recording of air and underwater acoustic signals.

At the beginning of every experiment, reference object was pictured to define real scale of the image.

The scheme of typical experiment is shown in Fig. 2.

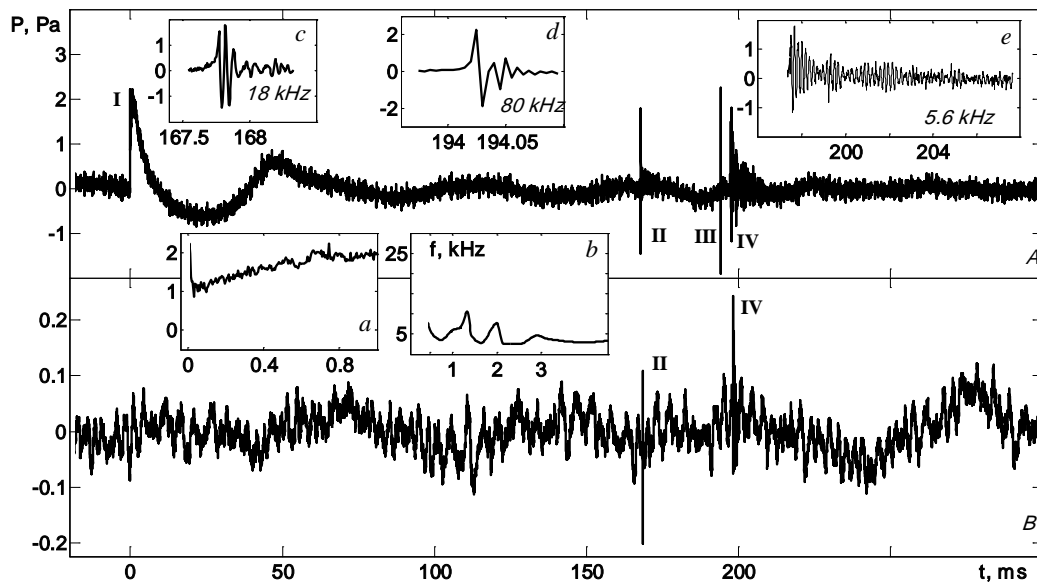


FIG. 3 HYDROPHONE (A) AND (B) MICROPHONE PHONOGRAMS. *a*) AND *b*) – SIGNAL I EXPANDED INITIAL PART AND ITS OSCILLATION FREQUENCY TIME DEPENDENCE. *c* – *e*) – EXPANDED SIGNALS II-IV. ORDINATES ARE IN Pa. ALL HORIZONTAL AXES ARE TIME IN ms. $U=2.6$ m/s, $We=460$, $Bo=3.3$, $Re=13000$, $Oh=0.002$

Sensitive element of the hydrophone was at depth h along the vertical of drop fall or at some displacement L_h .

The microphone head 4 was located at distance L_m in horizontal plane from drop impact point C (Fig. 2). The height of the microphone above the free surface was H_m . The microphone pattern axis forms an angle α with the vertical. The distance between the microphone and drop impact point C and difference in sound speeds in the air and underwater are the dominant causes of the delay the microphone signal with respect to hydrophone one.

Under the experiment conditions, altering of the dispenser height H enables implementation of various modes (We , Bo , Re) of impact that provides different scenarios of the flow evolution and acoustic emission. The mode with thick back jet ejecting large drops was selected as reach acoustic emission was fixed at this range of parameters in previous experiments due to entrainment of bubbles by drop impacts (Pumphrey H.C., Elmore P.A., 1990, Prosperetti A., Oguz H.N., 1993).

Basic Results

The result of experiment in which a droplet ($D = 0.5$ cm) fell from the altitude $H = 66$ cm and at the

moment of contact with the free surface had the velocity $U = 2.6$ m/s is shown in Fig. 3. The velocity was calculated from videorecords; calculated value differs from one derived without air drag taken into account (i.e., $U = \sqrt{2gH} = 3.6$ m/s). The experimental conditions correspond to dimensionless flow parameters $We = 608$, $Re = 15000$, $Bo = 3.3$, $Oh = 0.002$ at material parameters of the underlying liquid $\sigma = 74$ dyn/cm, $\nu = 0.01$ cm²s⁻¹, that provides the formation of both the sequence of caverns and the thick cumulative jet (Rein M., 1996). During evolution of primary and secondary caverns both isolated gas bubbles of various sizes and their groups aroused in the liquid. In addition, small gas bubbles grouped in annular structures within the drop fall area were observed, as in (Prosperetti A. Oguz H. N., 1993).

Sounding air bubbles tear themselves off the secondary caverns, and at the instant of detachment, they undergo extremely high accelerations initiating a resonant excitation of the bubbles (Prokhorov V.E., Chashechkin Yu. D., 2011a). However, the total number of bubbles is much more than a number of sound packets, so, only certain gas bubbles take part in sound emission.

Phonograms of the hydrophone and microphone are given on common time axis in Fig. 3. Difference in

noise levels reflects different scales of the outputs of hydrophone and microphone, respectively. The hydrophone output includes sharp initial pulse, low frequency oscillations caused by variation of free surface and three individual sound packets separated from initial pulse by time delays 170, 190 and 195 ms. The signal general structure corresponds to typical form observed before (Pumphrey H. C., Crum L.A., Bjorno L., 1989, Prokhorov V. E., Chashechkin Yu. D., 2011b). Microphone signal is poorer, and only two sound packets can be identified. This mismatch is conditioned by the microphone passband whose cut frequency is 40 kHz in contrast with 120 kHz of hydrophone.

The initial pulse I at the hydrophone output forms within a short time when droplet front edge penetrates into the free liquid surface. The pulse structure is visualized in the inset *a*. Its leading front with rate $0.5 \text{ Pa}/\mu\text{s}$ is accompanied with series of small oscillations whose internal frequency decreases non-monotonically with the time (inset *b*). Wide passband of the hydrophone allows tracing frequency variability within lifetime of the impact signal. The time is counted from the initial pulse everywhere here and below.

The next solitary packet II arises at 170 ms after initial pulse. The expanded plot of the II is given in the inset *c*. The signal spectrum is grouped near the frequency 18 kHz (Fig. 3, inset *c*). The signal II falls into passband of the microphone and appears at the microphone output, however, after 680 μs delay conditioned by propagation of the signals along the path $S_m = \sqrt{L_m^2 + H_m^2}$ in the air (Fig. 2).

In contrast, the packet III whose carried frequency is 80 kHz (inset *d*) is fixed only by the wide-band hydrophone.

The long-lived packet IV has the carried frequency 5.6 kHz and is fixed both in the air and underwater. The time dependence of the signal is given in the inset *e* where it looks like amplitude-modulated packet (carried frequency 5.6 kHz) slowly damping with time.

Overview of Fig. 3 shows that the succession of individual packets characterized by wide range of carried frequencies is emitted simultaneously in the air and underwater.

The next experiment shows that the main qualitative features of the signals are stable but individual packets parameters vary significantly even the drops are the same as can be seen from synchronous acoustic and optical records (Figs. 4 and 5).

At hydrophone output, four signals I – IV are fixed (Fig. 4). The initial pulse I associated with drop impact has front rate $1.5 \text{ Pa}/\mu\text{s}$.

Next signal II is weak and includes several packets, one with the highest frequency 67 kHz and the most pronounced another with 26 kHz (inset *a*). After a long silence (215 ms counting from impact signal I) intensive packet III appears and continues 31 ms. Then, after short pause (8 ms) a new packet 4 arises. Spectra of the packets III and IV are quite narrow as is shown in the inset *b*. Carried frequencies of the packets are 1.6 and 1.7 kHz, respectively.

The frames of the videorecords corresponding to the phonogram (Fig. 4) are shown in Fig. 5. Dark areas are images of the volumes filled with a gas. Complex shapes of gas cavities, their motion opposite buoyancy forces, and long lifetime of irregular shapes far from equilibrium forms show the existence of latent flow components. The flows occurred in a fluid bulk within domain of the drop initial contact and did not manifest themselves in displacement of the free surface.

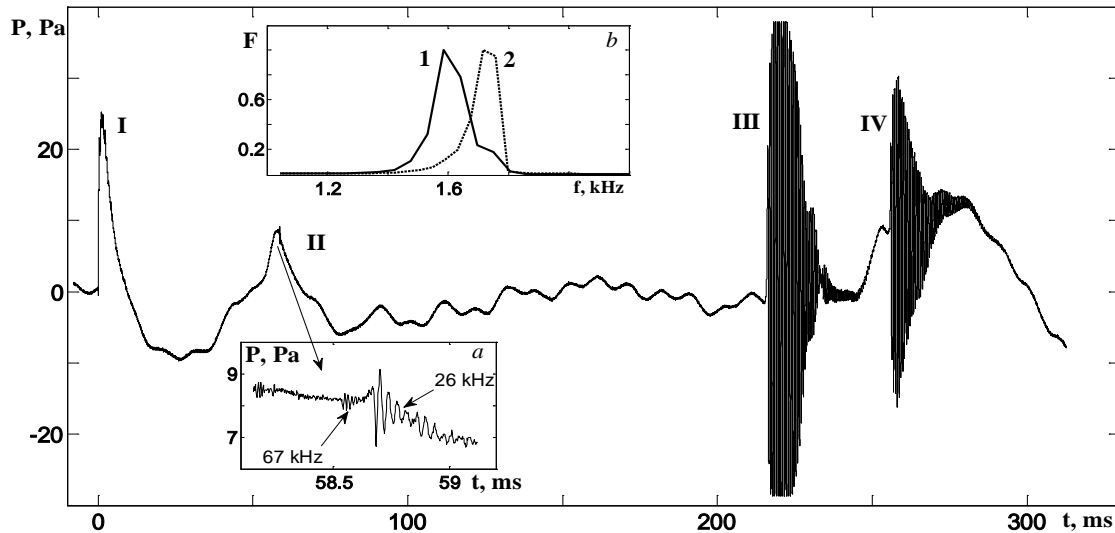


FIG. 4 SIGNAL AT THE HYDROPHONE OUTPUT FOR THE DROPLET FALL. THE LOW FREQUENCY OSCILLATIONS ARE ABOUT 48 Hz WITHIN $t = 70 - 190$ ms. (a) – EXPANDED SIGNAL II NEAR $t = 58.5$ ms, (b) – SPECTRA 1 AND 2 OF THE SOUND PACKETS III AND IV, RESPECTIVELY. $U = 3.4$ m/s, $We=780$, $Bo=3.3$, $Re=17000$, $Oh=0.002$.

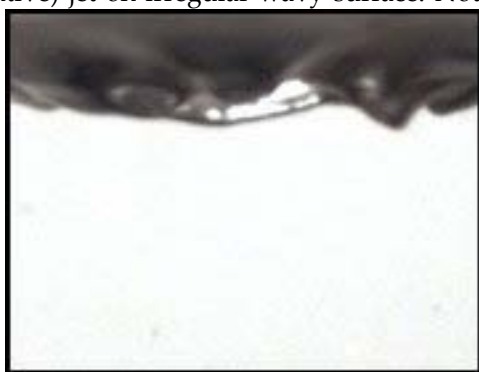
Upper part in Fig. 5a is remnant of initial cavern of which the low edge is covered by necklace of small gas bubbles as it was also observed in (Thoroddsen S.T., Etoh T. G, Takehara K., 2003).

The bubbles having different sizes create several weak sound packets of different carried frequencies (Fig. 4, inset a) which (26 and 67 kHz) differ more than in two and half times that is a consequence of the great difference in sizes of sounding bubbles. The bubbles having smooth shapes emit the sound of small intensities and short durations.

The large cavity of irregular shape in Fig. 5b formed after fall of the secondary drop torn off the tip of thick back (cumulative) jet on irregular wavy surface. Note

that the cavity is formed with very thin conic neck connecting it with remnant of the surface cavern (Fig. 5b). The flows entrained the cavity saving its irregular shape into the bulk of the fluid. Exactly this cavity is the source of intensive long-lived sound packet III (Fig. 4). The cavity is split into group of three new separated cavities of small sizes. Meanwhile, a newly formed cavern run up the group and touches them. The moment the cavern contacts the cavities the sounding stops (Fig. 5d).

New sound packet appears when the cylindrical neck between cavity and cavern is torn off with formation of two cross-counter sharp cones (Fig. 5e).



a



b

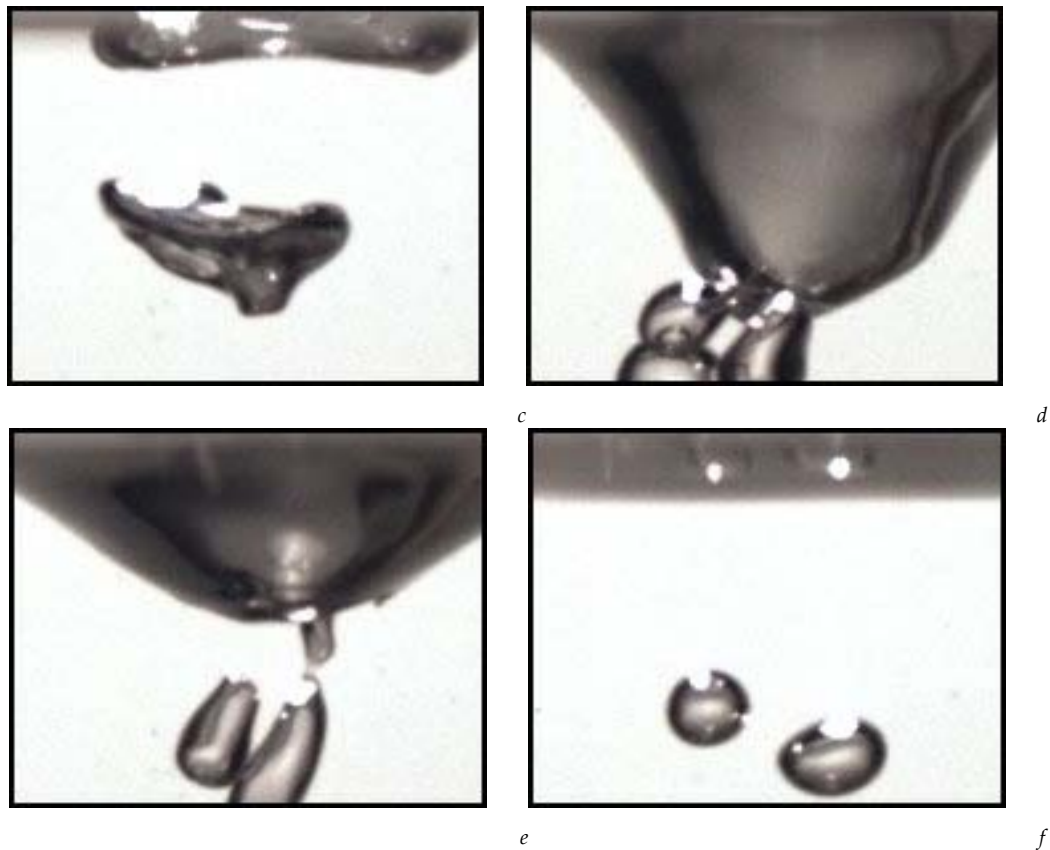


FIG. 5 FORMATION AND DETACHMENT OF THE AIR CAVITIES UPON DROPLET FALL: $t =$ (a) 58.7; (b) 215; (c) 223; (d) 246.5; (e) 255.7; AND (f) 284 ms.

Latent flows hold the cavities torn off on their initial horizons opposing the gravity forces. Initially the cavities have irregular shapes with sharp cone tips, but gradually their shapes approach the smooth equilibrium forms (Fig. 5f). Surface energy released due to shortening the cavity surface during smoothing its shape is transferred into emitted acoustic waves. The bubble of the equilibrium form stops sounding due to the lack of energy. The frequency of the sound is defined by size of the bubble in its equilibrium state, which depends on the volume of initial gas cavity.

Conclusions

The experiments were carried out with synchronous acoustic/video recording disclose key points of sound emission caused by drop impact.

The initial (shock) sound pulse arises at the instant of contact of the lower part of the drop with the concave surface of the accepting fluid. At the contact, a part of the free surfaces of the approaching fluids disappears. This leads to releasing of the surface internal energy forming a jump of the pressure. Releasing of the energy goes very fast as it occurs under the action of strong atomic and molecular forces. The pressure jump accelerates fluid particles forming the cavern

crown and creates initial (impact) sound pulse.

Next sound sources are the gas cavities detaching from the submerging caverns and having initially the strongly irregular forms with sharp cone tips. Sound emission occurs in the process of transformation of large initial surface into smaller final bubble surface with the internal energy released. In general, duration of sounding is defined by the time the cavity required to take a smooth (regular) shape, or until the cavity contacts another surface.

ACKNOWLEDGMENT

This work was supported in part by the Ministry of Education and Science of the Russian Federation (State contract no. 16.518.11.7059), the Program of the Russian Academy of Sciences Presidium P-23 "Fundamental Problems of Oceanology: Physics, Geology, Biology, and Ecology" and Russian foundation for basic research (Grant 12-01-00128-a).

REFERENCES

- Bjorno L. "Underwater rain noise: sources, spectra and interpretations". J. De Physique IV. Colloque C5. Supplement de J. De Physique 3 (1994): C5. 1023 – 1030.

- Chashechkin Yu.D., Prokhorov V.E. "The fine structure of a splash induced by a droplet falling on a liquid free surface at rest". *Doklady Physics* 56 (2011) no. 2: 134-139
- Crum L.A., Pumphrey H.C., Roy R.A., Prosperetti A. "The underwater sound produced by impacting snowflakes". *J. Acoust. Soc. Amer.* 106 (4) (1999): 1765-1770.
- Franz G.J. "Splashes as sources of sounds in liquids". *J. Acoust. Soc. Amer.* 31 (8) (1959): 1080-1096.
- Jones A.T., "The sound of splashes". *Science* 52 (1920):295-296.
- Guo Y.P., Ffowcs Williams J.E. "A theoretical study on drop impact sound and rain noise". *J. Fluid Mech.* 227 (1991): 345-355.
- Knudsen V.O., Alford R.S., Emling J.W. "Underwater ambient noise". *J. Marine Res.* 1 (1948): 410-428.
- Landau L.D., Lifshitz E.M. *Fluid Mechanics*. Vol. 6 (2nd ed.). Butterworth-Heinemann, 1987.
- Minnaert M. "On musical air bubbles and the sounds of running water". *Phil. Mag.* 16 (1933): 235-248.
- Nystuen J.A. "Rainfall measurements using underwater ambient noise". *J. Acoust. Soc. Amer.* 79 (1986): 972-982.
- Prosperetti A., Crum L.A., Pumphrey H.C. "The underwater noise of rain". *J. Geophys. Res.* 94 (C3) (1989): 3255-3259.
- Prosperetti A., Oguz H.N. "The impact of drops on liquid surfaces and the underwater noise of rain". *Annu. Rev. Fluid Mech.* 25 (1993): 577-602.
- Prokhorov V.E., Chashechkin Yu.D. "Sound generation as a drop falls on a water surface". *Acoustical Physics* 57 (2011a): 807-818.
- Prokhorov V.E., Chashechkin Yu.D. "Two Regimes of Sound Emission Induced by the Impact of a Freely Falling Droplet onto a Water Surface". *Doklady Physics* 56 (3) (2011b): 174-177.
- Prokhorov V.E., Chashechkin Yu.D. "Emission of the Sequence of Sound Packets during a Drop Falling onto the Surface of Water". *Doklady Physics* 57 (3) (2011c): 114-1118.
- Pumphrey H.C., Crum L.A., Bjorno L. Underwater sound produced by individual drop impacts and rainfall. ". *J. Acoust. Soc. Amer.* 85 (4) (1989): 518-1526.
- Pumphrey H.C., Elmore P.A. The entrainment of bubbles by drop impacts. *J. Fluid Mech.* 220 (1990): 539-567.
- Rayleigh. *The theory of sound*. London: Macmillan and co., 1877.
- Rein M. "The transitional regimes between coalescing and splashing drops". *J. Fluid. Mech.* 306 (1996): 145-165.
- Rogers V.B. "On the formation of rotating rings by air and liquids under certain condition of discharge". *Am. J. Sci. Arts. Second Series.* 26 (1858): 246-258.
- Thomson J.J., Newall H.F. "On the formation of vortex rings by drops falling into liquids and some allied phenomena". *Proc. R. Soc. London* 29 (1885): 417-436.
- Thoroddsen S.T., Etoh T.G, Takehara K. "Air entrapment under an impacting drop". *J. Fluid Mech.* 478 (2003): 125-134.
- Villermaux E., Bossa B. "Single-drop fragmentation determines size distribution of raindrops". *Nature Physics.* 5 (2009): 697-702.
- Wenz G. M. *Acoustic ambient noise in the ocean: spectra and sources*, *J. Acoust. Soc. Am.* 34, 1936-1956 (1962).
- Worthington A.M. *A study of splashes*. London, Longman & Green, 1908 (reprinted N.Y., Macmillan, 1963).